Reaction of $Pt_3(CO)_3(P\text{-}t\text{-}Bu_2Ph)_3$ and HCl. The X-ray Structure of $Pt_2Cl_2(CO)_2(P\text{-}t\text{-}Bu_2Ph)_2$

Christiane Couture, David H. Farrar,* Duncan S. Fisher, and Ravi R. Gukathasan

Department of Chemistry, Lash Miller Chemical Laboratories, University of Toronto, Toronto, Ontario, Canada M5S 1A1

Received July 11, 1986

The reaction of $Pt_3(CO)_3(P\text{-}t\text{-}Bu_2Ph)_3$ (1) with 3 equiv of HCl at −50 °C results in immediate formation of $PtHCl(CO)(P\text{-}t\text{-}Bu_2Ph)$ (2) in which the hydride ligand is assigned to the position trans to the CO ligand. Complex 2 isomerizes rapidly at higher temperatures to give a second complex, $PtHCl(CO)(P\text{-}t\text{-}Bu_2Ph)$ (3), with the hydride ligand trans to the chloride ligand. Complex 3 slowly converts to a dinuclear Pt(I) complex shown by X-ray crystallography to be $Pt_2Cl_2(CO)_2(P\text{-}t\text{-}Bu_2Ph)_2$ (4). Complex 4 crystallizes in the monoclinic space group $P2_1/c$ with $Z = 4$ in a unit cell of dimensions $a = 15.418$ (1) Å, $b = 14.751$ (1) Å, $c = 16.051$ (2) Å, and $\beta = 108.61$ (1)°. The structure was refined by using 4065 independent reflections with 203 variables to $R_1 = 0.046$ and $R_2 = 0.053$. 4 contains an unsupported Pt–Pt bond (2.628 (1) Å), and the phosphine ligands are located trans to this bond. The Pt atom coordination spheres are essentially square-planar with a dihedral angle of 109.9° between the two planes. The rotational energy of the Pt–Pt bond and the relative stability of 4 and a hypothetical Cl-bridged isomer are examined by using EHMO calculations. 4 also can be prepared by reacting 1.5 equiv of Cl_2 with 1 while reaction of 1 or 4 with excess Cl_2 gives $Pt(Cl)_2(CO)(P\text{-}t\text{-}Bu_2Ph)$ (7). Addition of excess $NaBH_4$ to a solution of 3 regenerates 1, and reaction of 3 with $AgPF_6$ gives $[(Pt_3(\mu\text{-}CO)_3(P\text{-}t\text{-}Bu_2Ph)_3)_2Ag][PF_6]$ (6). Complex 6 has been spectroscopically characterized as a Ag cation sandwiched between two units of 1. 6 is also the product of the reaction of 1 and $AgPF_6$.

Introduction

Transition-metal cluster compounds have been used as catalyst precursors in a number of homogeneously catalyzed reactions.[1,2] Clusters provide a potential source of very reactive mononuclear metal fragments that can become the active species in catalytic cycles. For example, $Fe_3(CO)_{12}$ reacts thermally with alkenes at 80 °C to form $Fe(CO)_4$(alkene) complexes that are catalytic intermediates in alkene isomerization.[3] Due to a specific interest in the breakdown of platinum cluster compounds into reactive mononuclear complexes[4] and a general interest in the chemistry of metal–hydrogen bonds, we have investigated the reaction of $Pt_3(CO)_3(P\text{-}t\text{-}Bu_2Ph)_3$ (1) and HCl. This reaction proceeds by fragmentation of the starting cluster to initially produce platinum(II) hydride complexes. Platinum(II) hydride complexes have played an important role in the development of transition-metal hydride chemistry. Many monohydridoplatinum(II) complexes of the type *trans*-$PtHXL_2$, where X = an anionic ligand and L = tertiary phosphines are known.[5,6] A few dihydridoplatinum(II) complexes, *trans*-PtH_2L_2 (L = bulky tertiary phosphines)[7] and *cis*-PtH_2L_2 (L = bulky chelating phosphines),[8,9] have been reported, but no neutral hydridoplatinum(II) complexes containing only one phosphine ligand have been reported.

Scheme I

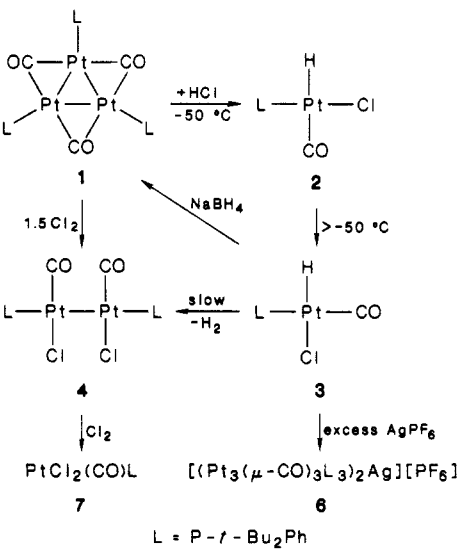

Results and Discussion

Reaction of $Pt_3(CO)_3(P\text{-}t\text{-}Bu_2Ph)_3$ and HCl. We have previously reported that the triplatinum cluster $Pt_3(CO)_3(P\text{-}t\text{-}Bu_2Ph)_3$ (1) undergoes rapid phosphine substitution by a pathway in which the metal triangle remains intact.[4] Reaction of 1 with small molecules such as CS_2 and SO_2 results in fragmentation to mononuclear products at low temperatures that then dimerize as the temperature is increased.[4] A similar process occurs when 1 is reacted with HCl, and the results of this study are summarized in Scheme I. It is convenient to add the HCl stoichiometrically as the amine adduct $MeCOMe_2NHCl$, although the same sequence of products is observed by using HCl gas. The reaction of 1 with 3 equiv of HCl, at −50 °C, results in immediate formation of $PtHCl(CO)(P\text{-}t\text{-}Bu_2Ph)$ (2) as the first observable intermediate. In complex 2 the hydride ligand is assigned to the position trans to the carbonyl ligand on the basis of the NMR coupling constants. The magnitude of the coupling constant between ^{31}P–^1H (12

(1) Johnson, B. F. G., Ed, *Transition Metal Clusters*. Wiley: New York, 1980.
(2) Wilkinson, G.; Stone, F. G. A.; Abel, E. W., Eds. *Comprehensive Organometallic Chemistry*; Pergaman Press: New York, 1982.
(3) Casey, C. P.; Cyr, C. R. *J. Am. Chem. Soc.* **1973**, *95*, 2248.
(4) Browning, C. S.; Farrar, D. H.; Gukathasan, R. R.; Morris, S. A. *Organometallics* **1985**, *4*, 1750 and references therein.
(5) Belluco, U. *Organometallic and Coordination Chemistry of Platinum*; Academic Press: New York, 1974.
(6) Hartley, F. R. *The Chemistry of Platinum and Palladium*; Halsted Press: New York, 1973.
(7) Goel, R. G.; Ogini, W. O.; Srivastava, R. C. *Organometallics* **1982**, *1*, 819.
(8) Moulton, C. J.; Shaw, B. L. *J. Chem. Soc., Chem. Commun.* **1976**, 365.
(9) Yoshida, T.; Yamagata, T.; Otsuka, S.; Tulip, T. H.; Ibers, J. A. *J. Am. Chem. Soc.* **1978**, *100*, 2063.

0276-7333/87/2306-0532$01.50/0

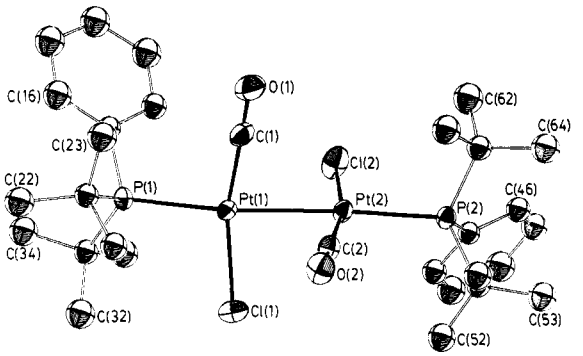

Figure 1. An ORTEP diagram of 4 with hydrogen atoms omitted. The thermal ellipsoids are represented by 30% probability contours.

Hz) and ^{13}C (CO)–^{1}H (75 Hz) in the initial mononuclear complex suggests that the hydride ligand is cis to the phosphine ligand and trans to the carbonyl ligand. Complete spectroscopic data for the complex **2** is reported in the Experimental Section. Due to the instability of the complex no analytical data could be obtained. Complex **2** is a kinetic product, and the cis relationship between the CO and P-*t*-Bu_2Ph ligands is consistent with the stereochemistry of **1**. The hydride ligand is cis to the P-*t*-Bu_2Ph ligand, which avoids placing these two strong σ-donor ligands opposite to each other. Complex **2** isomerizes rapidly, at temperatures between −50 and 0 °C, to give a second mononuclear complex, PtHCl(CO)(P-*t*-Bu_2Ph) (**3**), where the hydride ligand is trans to the weaker σ-donating chloride ligand. It appears that the isomerization is occurring for electronic reasons as this allows the hydride ligand to move cis to the two ligands with a high trans influence. It is assumed that the steric interactions between the P-*t*-Bu_2Ph ligand and a CO or a Cl^- ligand are comparable. A low coupling constant is observed between ^{31}P–^{1}H (14 Hz) and ^{13}C–^{1}H (3 Hz) while a higher value is found for ^{31}P–^{13}C (134 Hz). This complex, **3**, is stable in $CHCl_3$ for several hours, but all attempts to isolate it as a solid resulted in decomposition of the product. Complex **3** converts slowly over a period of approximately a week (in $CHCl_3$) to a dinuclear Pt(I) complex. The ^{31}P NMR spectrum of **4** indicates two chemically equivalent phosphine environments in a dinuclear complex. The IR spectrum has two strong absorbances at 2020 and 2040 cm^{-1}, suggesting that the terminal CO groups are bonded to Pt(I). These data do not permit unambiguous assignment of the structure, and thus an X-ray crystal structure determination was undertaken that revealed the complex to be $Pt_2Cl_2(CO)_2(P\text{-}t\text{-}Bu_2Ph)_2$ (**4**) as shown in Figure 1. The conversion of **3** into **4** is accompanied by release of H_2 as detected by gas chromatography. Binuclear reductive elimination of H_2 from platinum complexes has been reported previously.[10] The rate of this reaction is very solvent dependent; for example, in toluene the reaction is complete within a few hours whereas several days are required in $CHCl_3$. Complex **4** is the major decomposition product of **3** and is accompanied by small amounts ($\simeq$10%) of *trans*-PtHCl (P-*t*-$Bu_2Ph)_2$ (**5**) and traces (less than 5%) of an uncharacterized insoluble fraction. **5** can be prepared independently by the reaction of Pt(P-*t*-$Bu_2Ph)_2$ and HCl, and complete spectroscopic data for the compound are given in the Experimental Section.[11] The

Table I. Selected Bond Distances (Å) and Angles (deg)

Bond Distances			
Pt(1)–Pt(2)	2.628 (1)		
Pt(1)–Cl(1)	2.325 (3)	Pt(2)–Cl(2)	2.344 (3)
Pt(1)–P(1)	2.371 (3)	Pt(2)–P(2)	2.358 (3)
Pt(1)–C(1)	1.82 (1)	Pt(2)–C(2)	1.84 (1)
C(1)–O(1)	1.08 (1)	C(2)–O(2)	1.11 (1)
Bond Angles			
Pt(2)–Pt(1)–Cl(1)	85.99 (9)	Pt(1)–Pt(2)–Cl(2)	85.75 (8)
Pt(2)–Pt(1)–C(1)	79.1 (4)	Pt(1)–Pt(2)–C(2)	80.3 (3)
P(1)–Pt(1)–Cl(1)	98.5 (1)	P(2)–Pt(2)–Cl(2)	92.5 (1)
P(1)–Pt(1)–C(1)	96.8 (4)	P(2)–Pt(2)–C(2)	101.5 (3)
Pt(1)–C(1)–O(1)	179 (1)	Pt(2)–C(2)–O(2)	177 (1)

IR spectrum of the insoluble fraction has CO bands at 1880 and 2056 cm^{-1}, and the solid appears to be a mixture of products. We have no other information about this fraction.

Structure of $Pt_2Cl_2(CO)_2(P\text{-}t\text{-}Bu_2Ph)_2$. The crystals of **4** are built up from discrete molecules. The shortest contact between the molecules is 2.36 Å involving H(14) and H(622) at $(1 - x, -y, -z)$. A perspective view of the molecule together with the atom numbering scheme is given in Figure 1, and selected intramolecular distances are presented in Table I. Complex **4** consists of two distorted square-planar Pt(I) fragments held together by an unsupported Pt–Pt bond. The Pt–Pt bond distance, 2.628 (1) Å, is significantly longer than the value of 2.584 (2) Å reported for the related complex $Pt_2Cl_2(CO)_2(PPh_3)_2$.[12] This difference is ascribed to the stronger σ-donor strength of the P-*t*-Bu_2Ph ligand. The preparation of the complex $Pt_2Cl_2(CO)_2(PPh_3)_2$ and all other details of the crystal structure have not been published. In the only other neutral Pt(I) complex with an unsupported metal–metal bond, $Pt_2Cl_2(CN(2,4\text{-}t\text{-}Bu_2\text{-}6\text{-}MeC_6H_2))_4$, the Pt–Pt bond lengths are 2.563 (2) and 2.561 (2) Å (two independent molecules in the asymmetric unit).[13] The Pt–Pt distance in **4** is shorter than the values usually observed in Pt(0) complexes (2.65–2.79 Å) and within the range found for Pt(I) dimers (2.58–2.65 Å).[14] The largest deviation from a least-squares plane containing Pt(1) and its inner coordination sphere is 0.306 (3) Å (P(1)) while a distance of 0.176 (3) Å (P(2)) is found in the same calculation for Pt(2). A value of 70.1° was calculated for the dihedral angle between the two planes; the corresponding angle in $Pt_2Cl_2(CN(2,4\text{-}t\text{-}Bu_2\text{-}6\text{-}MeC_6H_2))_4$ is 88°.[13] The Pt(1) inner coordination sphere contains Cl(1), the phosphine ligand P atom P(1), the carbonyl ligand C atom C(1), and Pt(2). An equivalent inner coordination sphere exists at Pt(2). The angles subtended at both Pt atoms are consistent with a square-planar coordination geometry. Slight deviations from the ideal 90° angles are introduced by the steric demands of the phosphine ligands. The Pt–P distances are just significantly different, 2.371 (3) and 2.358 (3) Å for Pt(1) and Pt(2), respectively; no chemical significance is assigned to this difference. Both values are similar to the Pt–P distance of 2.349 (2) Å found in $Pt_2(CS_2)_2(P\text{-}t\text{-}Bu_2Ph)_2$.[15] The Pt–Cl values, 2.325 (3) and 2.344 (3) Å, are also slightly different but are comparable to other Pt–Cl bond lengths.[13,16,17] Both differences may

(10) (a) Minghetti, G.; Bandini, A. L.; Banditelli, G.; Bonati, F.; Szostak, R.; Strouse, C.; Knobler, C. B.; Kaesz, H. D. *Inorg. Chem.* **1983**, *22*, 2332. (b) Foley, H. C.; Morris, R. H.; Targos, T. S.; Geoffroy, G. L. *J. Am. Chem. Soc.* **1981**, *103*, 7337.
(11) Yoshida, T.; Otsuka, S. *J. Am. Chem. Soc.* **1977**, *99*, 2134.
(12) Boag, N. M.; Browning, J.; Crocker, C.; Goggin, P. L.; Goodfellow, R. J.; Murray, M.; Spencer, J. L. *J. Chem. Res., Synop.* **1978**, 228.
(13) Yamamoto, Y.; Takahashi, K.; Yamazaki, H. *Chem. Lett.* **1985**, 201.
(14) Dedieu, A.; Hoffmann, R. *J. Am. Chem. Soc.* **1978**, *100*, 2074.
(15) Farrar, D. H.; Gukathasan, R. R.; Morris, S. A. *Inorg. Chem.* **1984**, *23*, 3258.
(16) Farrar, D. H.; Ferguson, G. *J. Crystallogr. Spectrosc. Res.* **1982**, *12*, 465.

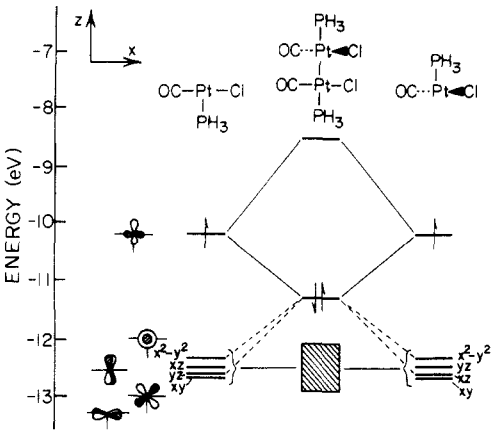

Figure 2. The interaction diagram of the frontier orbitals of two $PtCl(CO)(PH_3)$ fragments with a perpendicular geometry (C_2 symmetry). The block of the molecular orbital below the HOMO is a filled bonding and antibonding combination of d-type orbitals.

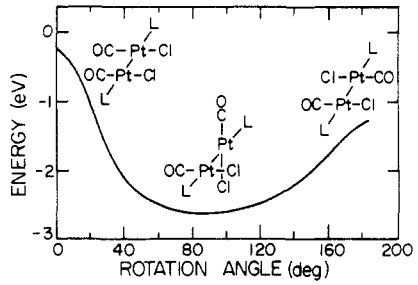

Figure 3. The energy profile for rotation about the Pt–Pt bond.

result from packing effects or may simply reflect an underestimation of the errors. The Pt–C(carbonyl) distances, 1.82 (1) and 1.84 (1) Å, are indistinguishable. The Pt–C(carbonyl) bond lengths reported for the dianion $[Pt_2Cl_4(CO)_2]^{2+}$ are 1.81 (2) and 1.78 (3) Å.[17] All parameters associated with the P-*t*-Bu_2Ph ligands are normal,[15] as are those of the carbonyl ligands.[17]

Using the extended Hückel molecular orbital method[18] and the fragment orbital formalism, we have carried out calculations on the simplified dimer $Pt_2Cl_2(CO)_2(PH_3)_2$ (**4a**). Figure 2 shows the interaction diagram of the frontier orbitals of two $PtCl(CO)(PH_3)$ fragments with a perpendicular geometry (C_2 symmetry). The frontier orbitals of the fragment are closely related to those of a square-planar PtL_3 fragment.[19] Figure 3 shows the energy profile for rotation about the Pt–Pt bond. The rotational barrier was evaluated to be 2.3 eV, which is less than the value 3.7 eV reported[13] for the related complex $Pt_2Cl_2(CN(2,4\text{-}t\text{-}Bu_2\text{-}6\text{-}MeC_6H_2))_4$ although energies from EHMO calculations are not reliable. The least stable configuration has C_{2v} symmetry with the Cl atoms eclipsed. Examination of the interaction diagram of the perpendicular configuration indicates that the metal–metal bond is of σ-symmetry arising from the combination of the two a′ orbitals in the $PtCl(CO)(PH_3)$ fragments (reduced Pt–Pt overlap population of 0.35) and therefore the rotational barrier should not arise from electronic factors. The barrier appears to come from steric interactions of the terminal chloride ligands. We have calculated a large negative reduced overlap population of −0.12 between the two chlorides in the eclipsed configuration; this number is interpreted as repulsion of the chloride filled p orbitals. The change in energy between 70 and 110° was less than 0.1 eV, and the dihedral angle in **4** lies just inside this range. The observed deviation of 19.9° from the ideal 90° dihedral angle may arise from the interaction of the Pt–Cl dipole moments that is consistent with the 88° dihedral angle in $Pt_2Cl_2(CN(2,4\text{-}t\text{-}Bu_2\text{-}6\text{-}MeC_6H_2))_4$ where the Cl^- ligands are trans to the Pt–Pt bond.

Some years ago a halogen-bridged dinuclear Pt(1) complex, $[Pt(\mu\text{-}I)(CO)(P\text{-}t\text{-}Bu_3)]_2$, was reported.[20] No structural data was obtained, but on the basis of ^{31}P NMR and IR spectroscopic results bridging iodides were inferred. The structure of this complex now should be assigned as the iodo analogue of complex **4** on the basis of the extreme similarities in the spectroscopic parameters. We have examined the bonding of a hypothetical chlorine-bridged dinuclear complex **4b**. The results suggest that the hypothetical isomer **4b** would be energetically unfavorable as the HOMO is antibonding in the bridging region and occupation of this molecular orbital would destabilize the complex. Removal of the two electrons from the HOMO should stabilize a chloride-bridged dimer, which is consistent with the known structure of platinum(II) halide-bridged dimers.[21] We have calculated that the chloride-bridged dimer **4b** is less stable than the complex having terminal ligands **4a** by about 6 eV. A detailed MO study[22] on related bridged dinuclear palladium(I) carbonyl chloride complexes has shown similar results.

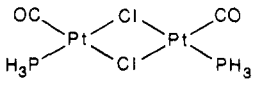

4b

Reactivity of 3 and 4. **3** is moderately stable at temperature below 0 °C, and we have studied some of the reactions of this complex. Addition of excess $AgPF_6$ to a THF solution of **3** produces a red solution from which a red-orange precipitate can be obtained. The precipitate has been characterized by NMR and IR spectroscopy and microanalysis as $([Pt_3(\mu\text{-}CO)_3(P\text{-}t\text{-}Bu_2Ph)_3)_2Ag][PF_6]$ (**6**). The ^{31}P NMR spectrum of **6** reveals that a basic Pt_3 framework is intact. The nuclearity and symmetry are evident in the Pt satellite resonances, which are similar to those observed in the spectrum of **1**. The ^{31}P–^{109}Ag (48.18%) and ^{107}Ag (51.82%) coupling are present in the ^{31}P NMR spectrum of **6**. The analytical data are consistent with the proposed structure of a Ag^+ ion sandwiched between the two Pt_3 triangles. The structure of the PPh-*i*-Pr_2 analogue of **6** has recently been determined, and the spectroscopic data reported for this complex are comparable with those of complex **6**.[23] Similar type metal complexes have been structurally characterized where Hg is bound between two Pt_3 triangles.[24,25] Complex **6** can be prepared directly by the reaction of **1** and $AgPF_6$. This observation suggests that the reaction of **3** and $AgPF_6$ proceeds by formation of **1**, which subsequently reacts with the silver salt. **1** could form from **3** and $AgPF_6$ if Cl^-

(17) Modinos, A.; Woodward, P. *J. Chem. Soc., Dalton Trans.* **1975**, 1516.
(18) (a) Hoffmann, R. *J. Chem. Phys.* **1963**, *39*, 1397. (b) Hoffmann, R.; Lipscomb, W. *Ibid.* **1962**, *36*, 2179. (c) Hoffmann, F.; Lipscomb, W. *Ibid.* **1962**, *37*, 2872.
(19) Albright, T. A.; Hoffmann, R.; Thibeault, J. C.; Thorn, D. L. *J. Am. Chem. Soc.* **1979**, *101*, 3801.
(20) Goel, A. B.; Goel, S. *Inorg. Nucl. Chem. Lett.* **1980**, *16*, 397.
(21) Cotton, F. A.; Wilkinson, G. *Advanced Inorganic Chemistry*; 4th ed.; Wiley-Interscience: New York, 1980; p 1069.
(22) Kostič, N. M.; Fenske, R. F. *Inorg. Chem.* **1983**, *22*, 666.
(23) Albinati, A.; Dahmen, K. H.; Togni, A.; Venanzi, L. M. *Angew. Chem., Int. Ed. Engl.* **1985**, *24*, 766.
(24) Albinati, A.; Moor, A.; Pregosin, P. S.; Venanzi, L. M. *J. Am. Chem. Soc.* **1982**, *104*, 7672.
(25) Yamamoto, Y.; Yamazaki, H.; Sakurai, T. *J. Am. Chem. Soc.* **1982**, *104*, 2329.

abstraction by Ag^+ is followed by reductive release of a proton and aggregation of the resulting $Pt(CO)(PtBu_2Ph)$ fragment.

Reaction of **3** and $NaBH_4$ produces **1**. This reaction is facile even at −50 °C, but we have observed a very unstable mononuclear intermediate by low-temperature ^{31}P NMR spectroscopy (δ 76.5 ($|^1J(P\text{–}Pt)|$ = 3097 Hz)) that is tentatively assigned as $PtH_2CO(P\text{-}t\text{-}Bu_2Ph)$. This complex could reductively eliminate dihydrogen to give complex **1**.[26]

3 reacts slowly with excess HCl yielding **5**, $PtCl_2(CO)(P\text{-}t\text{-}Bu_2Ph)$ (**7**), and traces of Pt metal. Complex **7** can be prepared by the reaction of **1** or **4** with excess Cl_2. Spectroscopic and analytical data for complex **7** are given in the Experimental Section. These observations are in agreement with the known reaction of $Pt_3(CO)_3(PR_3)_3$ and I_2.[20,27] The reaction of **4** and HCl results in oxidative addition across the Pt–Pt bond giving a 1:1 mixture of **3** and **7**.

Summary

Reaction of $Pt_3(CO)_3(P\text{-}t\text{-}Bu_2Ph)_3$ (**1**) with HCl initially gives a mononuclear product $PtHCl(CO)(P\text{-}t\text{-}Bu_2Ph)$ (**2**) where the H ligand is trans to the CO ligand, and this complex rearranges to the trans HCl isomer **3** before undergoing binuclear reductive elimination of H_2 to give $Pt_2Cl_2(CO)_2(P\text{-}t\text{-}Bu_2Ph)_2$ (**4**). **4** is susceptible to oxidative addition across the Pt–Pt bond.

Experimental Section

Infrared spectra were recorded on a Nicolet 5DX FTIR spectrometer. The ^1H, ^{13}C, and ^{31}P NMR were recorded on a Varian XL 200 spectrometer operating at 200, 50.3, and 81 MHz, respectively. The ^1H and ^{13}C chemical shifts were measured relative to an internal solvent reference and are reported relative to tetramethylsilane standard, while ^{31}P shifts were measured relative to external $P(OMe)_3$ in $CO(CD_3)_2$ and are reported relative to H_3PO_4. $P\text{-}t\text{-}Bu_2Ph$ and $Pt_3(CO)_3(P\text{-}t\text{-}Bu_2Ph)_3$ were synthesized by literature method.[11,28] Microanalysis were performed by Analytische Laboratorien, West Germany.

Synthesis of $PtHCl(CO)(P\text{-}t\text{-}Bu_2Ph)$ (2). $Pt_3(CO)_3(P\text{-}t\text{-}Bu_2Ph)_3$ (0.050 g, 0.037 mmol) and $MeCOMe_2NHCl$ (0.013 g, 0.11 mol) were dissolved in 1 mL of $CHCl_3$ (or $CDCl_3$) at −50 °C, and the NMR spectra showed **2** as the only product formed: ^{31}P NMR δ 63 ($|^1J(Pt\text{–}^{31}P)|$ = 3792 Hz); ^1H NMR δ −6.2 ($|^1J(Pt\text{–}^1H)|$ = 847 Hz, $|^2J(^1H\text{–}^{31}P)|$ = 12 Hz, $|^2J(^1H\text{–}^{13}C)|$ = 75 Hz).

Synthesis of $PtHCl(CO)(P\text{-}t\text{-}Bu_2Ph)$ (3). $Pt_3(CO)_3(P\text{-}t\text{-}Bu_2Ph)_3$ (0.050 g, 0.037 mmol) and $MeCOMe_2NHCl$ (0.013 g, 0.11 mmol) were dissolved in 2 mL of $CHCl_3$ at 0 °C. Within 2 min a green solution formed. NMR spectroscopy indicated that complex **3** was the major product present in the solution. All attempts to isolate a solid from the solution (for elemental analysis) were unsuccessful: ^{31}P NMR δ 60 ($|^1J(^{31}P\text{–}^{195}Pt)|$ = 3354 Hz); ^1H NMR δ −14.8 NMR δ ($|^1J(^1H\text{–}^{195}Pt)|$ = 1193 Hz, $|^2J(^1H\text{–}^{31}P)|$ = 14 Hz, $|^2J(^1H\text{–}^{13}C)|$ = 3 Hz, $|^2J(^{31}P\text{–}^{13}C)|$ = 134 Hz).

Synthesis of $Pt_2Cl_2(CO)_2(P\text{-}t\text{-}Bu_2Ph)_2$ (4). **3** was prepared in toluene, and the solution was stirred at 25 °C for 12 h. The solvent was removed at reduced pressure, and the resulting yellow solid was recrystallized from CH_2Cl_2/EtOH mixtures giving **4** in 60% yield: ^{31}P NMR δ 73 ($|^1J(^{31}P\text{–}^{195}Pt)|$ = 2381 Hz, $|^2J(^{31}P\text{–}^{195}Pt)|$ = 387 Hz, $|^4J(^{31}P\text{–}^{31}P)|$ = 202 Hz); IR ν(CO) 2020 (s), 2040 (s) cm^{-1}.

Method B. 1 (0.050 g, 0.037 mmol) and $C_6H_5ICl_2$ (0.015 g, 0.055 mmol) were dissolved in toluene, and the solution was stirred for 5 min. The solvent was removed at reduced pressure, and the resulting solid was recrystallized from CH_2Cl_2/EtOH as yellow crystals, yield 80%.

Table II. Crystal Data and Experimental Conditions Associated with Data Collection

mol formula	$C_{30}H_{46}O_2P_2Cl_2Pt_2$
fw	961.73
system	monoclinic
space group	$P2_1/c$
cell constants	
a, Å	15.418 (1)
b, Å	14.751 (1)
c, Å	16.051 (2)
β, deg	108.61 (1)
cell vol, Å^3	3459.9
D(calcd), g·cm^{-3}	1.85
Z	4
radiatn	Mo Kα, graphite monochromatized
μ(Mo Kα), cm^{-1}	84.34
wavelength, Å	0.71073
temp, °C	23
approximate cryst dimens, cm	0.015 × 0.006 × 0.011
no. and 2θ range of centered reflctns	25, $20 < 2\theta < 26°$
data collected	hkl and $hk\bar{l}$, for $0 < 2\theta < 50$
scan mode	$\theta/2\theta$
scan width, deg	0.75
max scan time, s	75
prescan rate, deg·min^{-1}	11
acceptance ratio $\sigma(I)/I$	0.04

X-ray Study of $Pt_2Cl_2(CO)_2(P\text{-}t\text{-}Bu_2Ph)_2$ (4). Yellow crystals of $Pt_2Cl_2(CO)_2(P\text{-}t\text{-}Bu_2Ph)_2$ were obtained by crystallization from CH_2Cl_2/EtOH mixtures. A photographic examination showed the crystals belonged to the monoclinic space group $P2_1/c$ (C_{2h}^5, No. 14).[29] Crystal data are presented in Table II.

A crystal was mounted on an Enraf-Nonius CAD4 diffractometer. Three standard reflections, monitored every 3.8 h, showed no decomposition had occurred during data acquisition. Details of the experimental conditions are summarized in Table II. The crystal faces were identified as {100}, {010}, (10$\bar{1}$), and ($\bar{1}$01). A total of 6305 reflections were measured. The recorded intensities were corrected for Lorentz and polarization effects, and a standard deviations $\sigma(I)$ was assigned to each intensity (I), using the data reduction program of the Enraf-Nonius SDP package.[30] Of the unique data collected, 4065 data with $I > 3\sigma(I)$ were available for the determination of the structure.

The positional coordinates for the Pt atoms were obtained from a three-dimensional Patterson synthesis. A series of difference Fourier syntheses and least-squares refinements revealed the positions of the remaining 36 non-hydrogen atoms. The data were corrected for absorption using the Gaussian method (8 × 4 × 14 grid). Transmission coefficients varied from 0.232 to 0.367. H atoms were located and were included in subsequent calculations with idealized positional coordinates (either sp^2 or sp^3 (staggered) geometries and a C–H bond distance of 0.95 or 1.0 Å, respectively) but not refined. After several cycles of full-matrix least-squares refinement on F the model converged at $R_1 = \sum||F_c| - |F_o|/\sum|F_o|| = 0.0457$ and $R_2 = (\sum w(|F_c| - |F_o|)^2/\sum wF_o^2) = 0.0533$ (4065 observations and 203 variables, Pt, Cl, P, and the carbonyl C and O atoms refined with anisotropic thermal parameters and all remaining C atoms refined isotropically). In the final cycle no shift exceeded 0.02 of its standard deviation. A total difference Fourier synthesis calculated from the final structure factors contained no features of chemical significance with the highest peak, of electron density 2.09 e·Å^{-3}, associated with the Pt(2) atom at fractional coordinates (0.771, −0.043, 0.293). The error in an observation of unit weight is 1.29. Final positional and B(iso) thermal parameters for the non-H atoms are given in Table III. The anisotropic thermal parameters, H-atom parameters, some least-squares planes, the bond distances and angles for the P-t-

(26) Anderson, G. K.; Clark, H. C.; Davies, J. A. *Organometallics* **1982**, *1*, 550 and references therein.
(27) Clark, H. C.; Goel, A. B.; Wong, C. S. *Inorg. Chim. Acta* **1979**, *34*, 159.
(28) (a) Field, M.; Stelzer, O.; Schmutzler, R. *Inorg. Synth.* **1973**, *14*, 4. (b) Mann, B. E.; Shaw, B. L.; Slade, R. M. *J. Chem. Soc. A* **1971**, 2976. (c) Hoffman, B. H.; Schellenbeck, P. *Chem. Ber.* **1967**, *100*, 692.
(29) *International Tables for X-ray Crystallography*; Kynoch Press: Birmingham, England, 1969; Vol. 1.
(30) All calculations were performed by using the Enraf-Nonius Structure Determination Package running on a DEC PDP-11/23 computer.

Table III. Positional and Thermal Parameters (Å²) for the Non-Hydrogen Atoms[a]

atom	x	y	z	B(iso)
Pt(1)	0.72096 (3)	0.09880 (3)	0.31126 (3)	3.158 (9)
Pt(2)	0.82165 (3)	−0.02013 (3)	0.26176 (3)	3.21 (1)
Cl(1)	0.7568 (3)	0.0166 (3)	0.4415 (2)	6.2 (1)
Cl(2)	0.6830 (2)	−0.0749 (3)	0.1658 (3)	5.82 (9)
P(1)	0.6100 (2)	0.1973 (2)	0.3357 (2)	3.19 (7)
P(2)	0.9066 (2)	−0.1366 (2)	0.2235 (2)	3.13 (7)
O(1)	0.7158 (7)	0.1749 (7)	0.1429 (6)	7.0 (3)
O(2)	0.9676 (6)	0.0842 (6)	0.3906 (6)	5.9 (3)
C(1)	0.7186 (8)	0.1458 (9)	0.2057 (8)	4.5 (3)
C(2)	0.9126 (8)	0.0437 (8)	0.3436 (8)	4.1 (3)
C(11)	0.5184 (8)	0.2150 (8)	0.2308 (7)	3.8 (2)
C(12)	0.5025 (8)	0.1448 (9)	0.1685 (8)	4.3 (3)
C(13)	0.433 (1)	0.150 (1)	0.0900 (9)	5.9 (3)
C(14)	0.380 (1)	0.225 (1)	0.0721 (9)	6.1 (3)
C(15)	0.393 (1)	0.295 (1)	0.1305 (9)	6.1 (3)
C(16)	0.463 (1)	0.289 (1)	0.2100 (9)	5.5 (3)
C(21)	0.6651 (8)	0.3103 (8)	0.3729 (7)	3.9 (3)
C(22)	0.612 (1)	0.376 (1)	0.4116 (9)	5.9 (3)
C(23)	0.683 (1)	0.356 (1)	0.2951 (9)	6.0 (3)
C(24)	0.7582 (9)	0.291 (1)	0.4446 (8)	5.0 (3)
C(31)	0.5435 (8)	0.1534 (9)	0.4071 (7)	4.0 (3)
C(32)	0.603 (1)	0.151 (1)	0.5043 (9)	5.7 (3)
C(33)	0.5130 (9)	0.059 (1)	0.3741 (8)	5.0 (3)
C(34)	0.458 (1)	0.210 (1)	0.3992 (9)	5.7 (3)
C(41)	0.8437 (7)	−0.2445 (8)	0.2077 (7)	3.4 (2)
C(42)	0.7956 (8)	−0.2628 (9)	0.2652 (7)	4.2 (3)
C(43)	0.753 (1)	−0.347 (1)	0.2637 (9)	5.7 (3)
C(44)	0.754 (1)	−0.409 (1)	0.201 (1)	6.2 (4)
C(45)	0.7973 (9)	−0.3917 (9)	0.1411 (8)	4.9 (3)
C(46)	0.8431 (8)	−0.3079 (9)	0.1450 (8)	4.2 (3)
C(51)	1.0147 (8)	−0.1700 (9)	0.3160 (7)	3.9 (2)
C(52)	0.9909 (9)	−0.178 (1)	0.3985 (9)	5.4 (3)
C(53)	1.0507 (9)	−0.263 (1)	0.2965 (9)	5.7 (3)
C(54)	1.089 (1)	−0.096 (1)	0.3266 (9)	5.3 (3)
C(61)	0.9319 (8)	−0.1034 (9)	0.1213 (8)	4.2 (3)
C(62)	0.842 (1)	−0.111 (1)	0.042 (1)	6.3 (4)
C(63)	0.962 (1)	−0.003 (1)	0.1306 (9)	5.8 (3)
C(64)	1.006 (1)	−0.158 (1)	0.0980 (9)	6.0 (3)

[a] Estimated standard deviations in the least significant figure(s) are given in parentheses. Anisotropically refined atoms are given in the form of the isotropic equivalent thermal parameter defined as $(^4/_3)[a^2B(1,1) + b^2B(2,2) + c^2B(3,3) + ab(\cos\gamma)B(1,2) + ac(\cos\beta)B(1,3) + bc(\cos\alpha)B(2,3)]$.

Bu_2Ph ligands, and the structure amplitudes have been deposited as supplementary material.

Synthesis of *trans*-PtHCl(P-*t*-Bu_2Ph)$_2$ (5).[11] Pt(P-*t*-Bu_2Ph)$_2$ (0.100 g) was dissolved in oxygen-free hexanes, and HCl was bubbled through the solution. After 5 min the white precipitate was obtained by filtration; yields are quantitative; ^1H NMR δ −18.44 ($|^1J(^1H-^{195}Pt)|$ = 1199 Hz; ^{31}P NMR δ 63.1 ($|^1J(^{31}P-^{195}Pt)|$ = 3058 Hz, $|^2J(^1H-^{31}P)|$ = 12 Hz). Anal. Calcd for $PtP_2ClC_{28}H_{47}$: C, 50.1; H, 7.0; Cl, 4.6; P, 9.2. Found: C, 49.6; H, 7.0; Cl, 5.0; P, 9.0.

Synthesis of [($Pt_3(\mu$-CO)$_3$(P-*t*-$Bu_2Ph)_3)_2Ag$][PF_6] (6). 3 (0.080 g, 0.17 mmol) and $AgPF_6$ (0.045 g, 0.18 mmol) were stirred together in 5 mL of THF. Within 5 min a red solution appeared from which a red product was isolated after removal of the solvents under reduced pressure. The solid was recrystallized with CH_2Cl_2/hexanes to give red-orange crystals; yield 95%; ^{31}P NMR δ 81.5 ($|^1J(^{31}P-^{195}Pt)|$ = 5555 Hz, $|^2J(^{31}P-^{195}Pt)|$ = 329 Hz, $|^3J(^{31}P-^{195}Pt)|$ = 22 Hz, $|^2J(^{31}P-^{107}Ag)|$ = 34 Hz, $|^2J(^{31}P-^{109}Ag)|$ = 37 Hz); IR ν(CO) 1813 (s), 1774 (w) cm^{-1}.

Synthesis of $PtCl_2$(CO)(P-*t*-Bu_2Ph) (7). 1 (0.070 g, 0.05 mmol) was dissolved in CH_2Cl_2, and the solution was cooled to 0 °C. Cl_2 was passed through the solution for 2 min. The solvents were then removed under reduced pressure to give a yellow product that was washed with hexanes; yield 95%; ^{31}P NMR δ 46.8 ($|^1J(^{31}P-^{195}Pt)|$ = 3035 Hz); IR ν(CO) 2105 (s) cm^{-1}. Anal. Calcd for $PtPCl_2OC_{15}H_{23}$: C, 34.9; H, 4.5. Found: C, 34.8; H, 4.5.

Reaction of 4 with HCl. HCl gas was bubbled through a solution of 4 (0.080 g, 0.083 mmol) in CH_2Cl_2 at 0 °C for 1 min. The solvents were removed at reduced pressure, and ^{31}P NMR spectroscopy revealed a 1:1 mixture of 5 and 7 with traces (less than 1%) of 2 and 3.

Reaction of 4 with Cl_2. As above with Cl_2 gas replacing HCl gas produces 7 as the only observable product.

Details of the EHMO Calculations. EHMO calculations[18] were carried out on the simplified complex [Pt(Cl)(CO)$(PH_3)]_2$ with interatomic distances based on the X-ray crystal structure of 4 with a geometry idealized to square-planar for each Pt center: Pt–Pt, 2.62 Å; Pt–P, 2.37 Å; Pt–Cl, 2.30 Å; Pt–C, 1.80 Å; C–O, 1.10 Å; P–H, 1.40 Å; Pt–P–H, 110°. The dihedral angle θ between the two square-planar PtL_3 fragments was varied from 0 to 180° (from C_{2v} to C_{2h} symmetry). For the complex [Pt(μ-Cl)(CO)$(PH_3)]_2$, the calculations were done by using the following structural parameters: Pt–Pt, 2.72 Å; Pt–Cl, 2.37 Å; Pt–Cl–Pt, 70°; P–Pt–C, 80°; the remaining parameters are the same as mentioned above. Values for H_{ii} and orbital exponents were taken from the ref 31.

Acknowledgment. We thank the Natural Sciences and Engineering Council of Canada for operating and equipment grants and Johnson Matthey and Co. Ltd for their loan of Pt salts. We also thank N. Plavac for his technical assistance in recording the NMR spectra.

Supplementary Material Available: Tables of anisotropic thermal parameters, derived hydrogen atom parameters, weighted least-squares planes, and distances and angles for the P-*t*-Bu_2Ph ligands (5 pages); a listing of structure factor amplitudes (21 pages). Ordering information is given on any current masthead page.

(31) Summerville, R. H.; Hoffmann, R. *J. Am. Chem. Soc.* **1976**, *98*, 7240.